NANO LETTERS

2002
Vol. 2, No. 10
1055−1060

Template Guided Self-Assembly of [Au_{55}] Clusters on Nanolithographically Defined Monolayer Patterns

Shantang Liu,[†] Rivka Maoz,[†] Günter Schmid,[‡] and Jacob Sagiv*,[†]

Department of Materials and Interfaces, The Weizmann Institute of Science, Rehovot 76100, Israel, and Institute of Inorganic Chemistry, University of Essen, Universitätsstrasse 5-7, 45117 Essen, Germany

Received June 20, 2002; Revised Manuscript Received August 4, 2002

ABSTRACT

Planned nanopatterns of [$Au_{55}(Ph_2PC_6H_4SO_3Na)_{12}Cl_6$] clusters are generated on smooth silicon surfaces using a "bottom-up" fabrication methodology based on the selective self-assembly of the gold clusters on purpose-designed organic template patterns themselves fabricated via a hierarchical layer-by-layer self-assembly strategy. The patterns are laterally defined by constructive nanolithography, a novel surface patterning process utilizing conductive AFM tips as nanoelectrochemical "pens", with which nanoscale chemical information is inscribed in a nondestructive manner (in the form of a localized chemical transformation) on the top surface of a highly ordered organosilane monolayer self-assembled on silicon. Development of the initial tip-imprinted information is achieved via further self-assembly and chemical derivatization steps. This generic all-chemical approach offers attractive options for the advancement of nanofabrication capabilities that might have real impact on future technologies.

Metal and semiconductor nanoparticles exhibit quantized electrical and optical properties that might be advantageously exploited in the design of future nanodevices. For example, sufficiently small metal particles are particularly attractive for applications such as quantum dots in "single electron" devices operating at the ambient temperature.[1,2] To materialize these prospects, it will, however, be necessary to advance nanofabrication capabilities enabling both the reproducible synthesis of particles with the required composition and size and their reliable assembly into surface-immobilized structural units specifically designed for the desired purpose. [Au_{55}] denotes a family of ligand-stabilized gold clusters ideally suited for such applications,[2,3] each cluster representing a well defined gold "supramolecule" with a metal core made of only 55 atoms (∼1.4 nm diameter) and an organic ligand shell that can be engineered such as to confer variable chemical and structural characteristics to the metal particle.[2−6] Considerable research efforts have, therefore, been invested in devising ways that would allow the deliberate organization of [Au_{55}] clusters into various surface-immobilized structural motifs of interest.[5] Using different procedures, both two-dimensional and one-dimensional arrangements of such clusters could be realized[5−7] and the electrical behavior of some of them studied;[5,8] however, the advancement of a reliable metal cluster assembly methodology that is potentially useful for nanodevice fabrication remains a challenging task.

Nanofabrication is one of the most complex basic problems nanoscience faces today. The great promise of nanoscience ultimately depends on our ability to organize matter on the nanoscale so as to create planned functional assemblies that not only display desirable properties but are also sufficiently stable and can be accurately reproduced. How to reach this goal is still a matter of considerable uncertainty and controversy, which further complicates the problem and turns it into an even more challenging one. Although a "bottom-up" chemical approach appears inherently well suited for the rational handling of nano- and subnanosize entities, there are no obvious chemical routes to be pursued, and the advancement of such a sufficiently general approach is still in its infancy. Ongoing research efforts in this direction have recently led to the development of a promising generic methodology for the planned assembly of hybrid organic−inorganic nanoscale architectures, based on processes of surface chemical derivatization and guided self-assembly taking place on well-defined organic template scaffolds, themselves produced via a hierarchical layer-by-layer self-assembly strategy.[9,10] According to this methodology, template patterns of any arbitrary design may, in principle, be generated by a novel two-dimensional (2D) patterning process, referred to as "constructive nanolithography",

* Corresponding author: Phone: +972-8-9342309; Fax: +972-8-9344138; E-mail: jacob.sagiv@weizmann.ac.il.
[†] The Weizmann Institute of Science.
[‡] University of Essen.

10.1021/nl025659c CCC: $22.00
Published on Web 08/20/2002

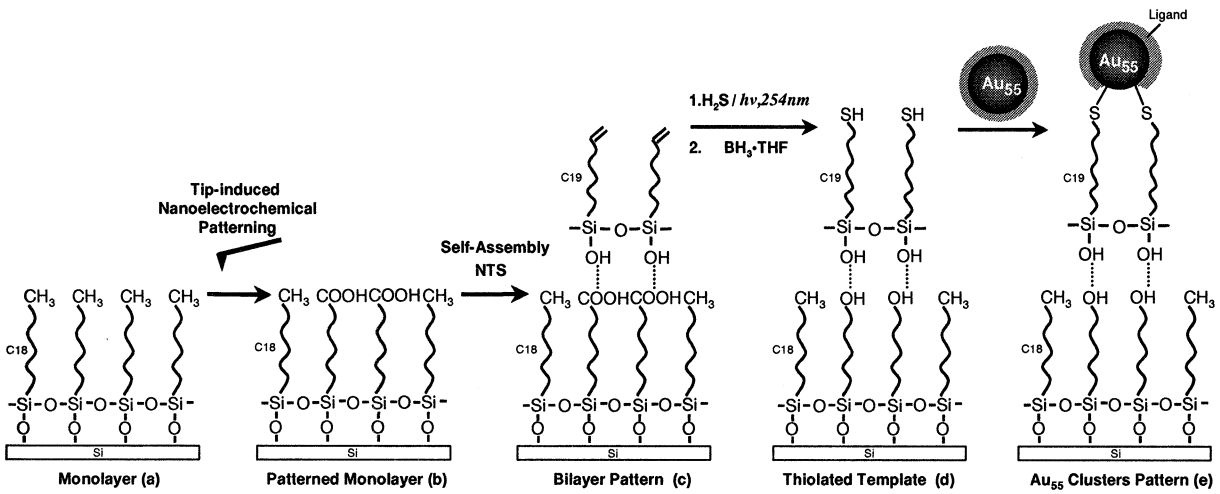

Figure 1. Schematic representation of the fabrication of an organosilane template pattern with top thiol functionality and the selective self-assembly of [Au_{55}] clusters on the template (see text). This sketch (not drawn to scale) emphasizes some of the salient features of the investigated system that are of direct relevance to the present study; it is not to be construed as representing a real structural model.[13]

whereby electrical pulses delivered by a conductive atomic force microscope (AFM) tip induce local electrochemical transformations, selectively affecting the top functions of a highly ordered organosilane monolayer self-assembled on silicon.[9,10] When operated in this mode, the scanning tip becomes a versatile nanoelectrochemical "pen" with which nanoscale chemical information is inscribed in a nondestructive manner on the top surface of the patterned organic monolayer. The initial tip-imprinted information can be further developed in a predictable manner, by the application of a rich menu of post-patterning surface chemical derivatization and self-assembly steps.[10] Proper planning and optimization of the overall process are required to ultimately realize the desired nanostructure. This approach was recently applied to the in-situ surface generation of metal and semiconductor nanosize features such as conducting silver wires and arrays of CdS nanoparticles, the latter being further converted to gold via a redox chemical process.[11]

Here we report a series of preliminary experimental results demonstrating a different possible mode of template-guided assembly of gold nanostructures on silicon, via surface import of ex-situ synthesized [Au_{55}] clusters and their spontaneous organization on organic template patterns defined by constructive nanolithography. Using ex-situ synthesized gold clusters with well-defined size and composition offers the advantage that such metal species may serve as known standards for both size calibration and in the electrical characterization of the surface-generated metal features.

In this study we explored the organization of the water-soluble derivative $[Au_{55}(Ph_2PC_6H_4SO_3Na)_{12}Cl_6]^2$ on bilayer template patterns with top thiol (−SH) functionality. It was anticipated that a mechanism of ligand exchange[2,12] would drive the specific adherence of the gold clusters to the thiolated template sites. The overall fabrication process, depicted schematically in Figure 1, starts with the tip-induced nanoelectrochemical inscription of the desired pattern of carboxylic acid (COOH) groups on the top surface of a highly ordered OTS (C18, *n*-octadecyltrichlorosilane) monolayer self-assembled on the entire surface of a silicon wafer substrate (a → b).[10,11,14] Subsequent exposure of the patterned OTS surface to a solution of NTS (C19, nonadecenyltrichlorosilane) results in the selective self-assembly of a monolayer with terminal ethylenic functions (−CH═CH_2) on the tip-inscribed sites (b → c).[10,11,13] Photochemical radical addition of H_2S to the reactive ethylenic functions of NTS and further reduction (with BH_3·THF) of the fraction of disulfide (−S−S−) groups produced in the process[10,11,15] effect the conversion of NTS to a fully thiolated overlayer copy of the initial pattern of carboxylic acid groups (c → d).[10,11] Finally, the formation, on the thiolated bilayer template, of a pattern of surface immobilized gold clusters is completed with the exposure (for ∼12 h) of the silicon wafer specimen to a dilute (5×10^{-5} M) aqueous solution of [Au_{55}], followed by copious rinse (∼4 min overflow) with pure water (d → e).[16]

A number of representative examples of planned patterns of gold clusters fabricated by the present method are given in Figures 2−5. These include different geometrical shapes, with lateral dimensions in the range between ∼10 nm to 2000 nm, which serve to illustrate some apparent aspects of the mode of organization of [Au_{55}] on the organic template. In all cases, the anchoring of the clusters to the surface is seen to faithfully follow the initial tip-inscribed patterns, thus confirming the validity of the hierarchical step-by-step assembly strategy outlined in Figure 1. Besides structural robustness,[16] these gold/template composite nanoarchitectures also exhibit good thermal stability, virtually identical AFM images[17] being obtained before and after 12 h of thermal annealing in vacuum (∼10^{-9} Torr), first at a temperature of 80 °C and then at 120 °C (Figures 2−5). X-ray photoelectron spectroscopic (XPS) data obtained from unpatterned [Au_{55}]/thiolated bilayer template samples produced on large-area Si substrates by an analogous experimental procedure reveal the presence of phosphorus on the surface, in addition to that of the other expected elements (Au, S, C, Si, and O). This suggests that the initial phosphine ligand shell is only partially lost (as indicated in the illustration of Figure 1, e) in the exchange process effecting the attachment of the gold clusters to the thiolated surface.

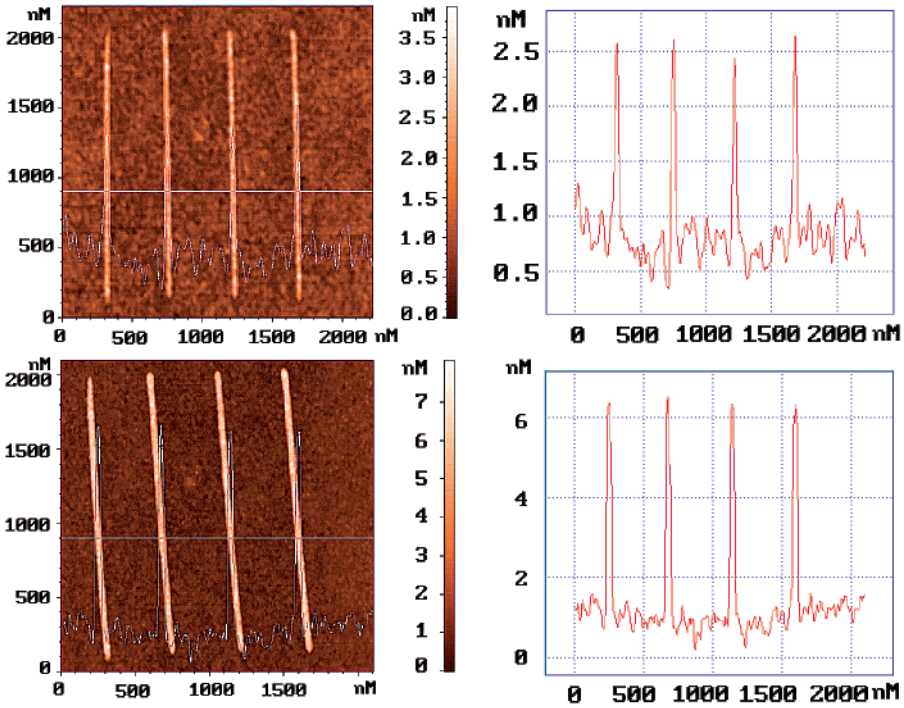

Figure 2. AFM semicontact mode topographic images of a pattern of parallel wires (inscribed in the vector mode[14]), and distance-height profiles along the marked lines, taken (top image) after the assembly of the bilayer pattern (step c in Figure 1), and (bottom image) after the final assembly of [Au_{55}] on the thiolated template (step e in Figure 1) and further annealing at 80 °C for 12 h (see text). The size of the deposited gold particles is evaluated from the difference between the measured wire heights in the two images.

A comparative analysis of the AFM images of the different fabricated patterns reveals the deposition of a single layer of gold particles on most of the template surface. Larger features, possibly formed by the coalescence of two or more clusters (in solution or/and on the surface), are evident at isolated surface spots and represent only a small fraction of the total gold covered area. There is good agreement between the apparent size of individual particles as derived from images of different patterns, or images of the same pattern taken at variable magnifications, before and after thermal annealing, and with different probes; observed heights are in the range 3.0−3.6 nm (Figure 2), and lateral dimensions vary between 10 and 16 nm (Figures 3−5). Considering the rather uniform size of most of the individual particles distinguishable in Figures 3−5, and the apparent preservation of the protecting ligand shell (as indicated by the XPS data) on the outer surface of the template bound particles, we can rule out the possibility that these are actually larger gold aggregates formed on the surface by the coalescence of several ligand-depleted [Au_{55}] clusters. This would imply the existence of a rather improbable aggregation mechanism, whereby a fixed number of [Au_{55}] clusters participate in the formation of each surface bound gold particle. It is well known that AFM tends to overestimate lateral dimensions, because of the convolution with the tip.[18] Systematic deviations may, however, also affect the accuracy of height measurements if surface forces vary from spot to spot, for example, when images of objects made of soft and hard materials, or displaying different adhesion and hydration properties, are simultaneously acquired.[19] The systems presently investigated are highly heterogeneous in this respect; the gold clusters (a composite material made of a hard metal core and a soft organic shell) reside on top of elevated organic bilayer regions with hydrophilic top chemical functionality, surrounded by a hydrophobic monolayer background. Thus, the expected artifactal nature of the AFM height determinations under such conditions may explain the discrepancy between the present derived figures (3.0−3.6 nm) and the characteristic size (2.3−2.4 nm) of [Au_{55}] obtained from TEM[6,20] and X-ray diffraction[20] data.

It follows from this analysis (also considering the quasi-spherical geometry of [Au_{55}]), that, in general, we may not expect to see well resolved individual particles in AFM images of closely packed arrangements of such clusters. This implies that the rather well resolved 2D arrangement of particles in Figure 3 is actually less dense than it may appear. A somewhat higher local particle density is apparent in the array of dots in Figure 4. Here, a small number (2−5) of partially resolved clusters are seen to have assembled on each template dot with an apparent lateral size of 30−50 nm. The assembly on the wire templates gave rise to an even higher local density of gold clusters. While no details are distinguishable in the low resolution image of the four wires shown in Figure 2, magnified views of limited portions of the same wires clearly indicate (Figure 5, b and d) that the gold clusters are arranged in two densely packed parallel rows. As each wire has an apparent total width of the order of 30 nm, (Figures 2 and 5, a and c), the preferred organization of the clusters seems to be such that they concentrate at the periphery of the template, leaving a gap narrower than the size of one cluster (ca. 1/3 of the apparent total width of the wire) in its center. Finally, the assembly of planned

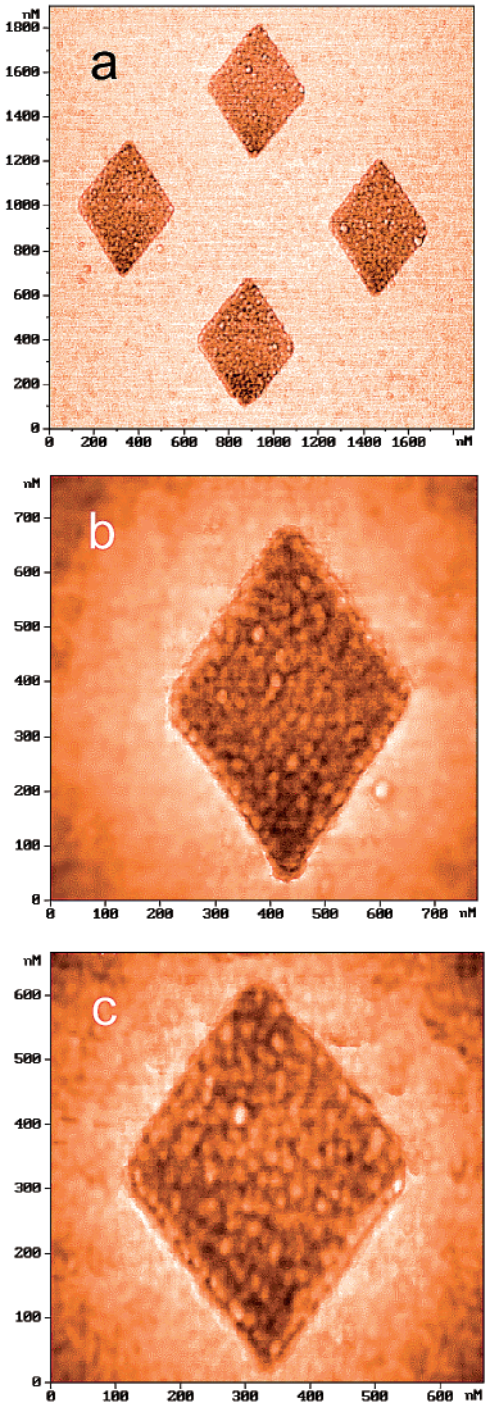

Figure 3. AFM semicontact mode phase images of (a) as-fabricated pattern of four [Au_{55}]/thiolated bilayer rhombuses (structure as in Figure 1e), (b) enlarged scan of the left-side rhombus after annealing at 80 °C for 12 h, (c) enlarged scan of the upper rhombus after annealing at 80 °C and then at 120 °C for 12 h (see text). The isolated larger features observed near the lower right side of rhombus b and within rhombus c, near its upper left side, are not gold features, as they also appear in the corresponding images of the bilayer pattern acquired before the assembly of the gold particles. These may represent structural irregularities induced by defects in the underlying substrate surface.

architectures combining several different structural elements of possible relevance to the future realization of certain types of single electron devices was also examined. For example,

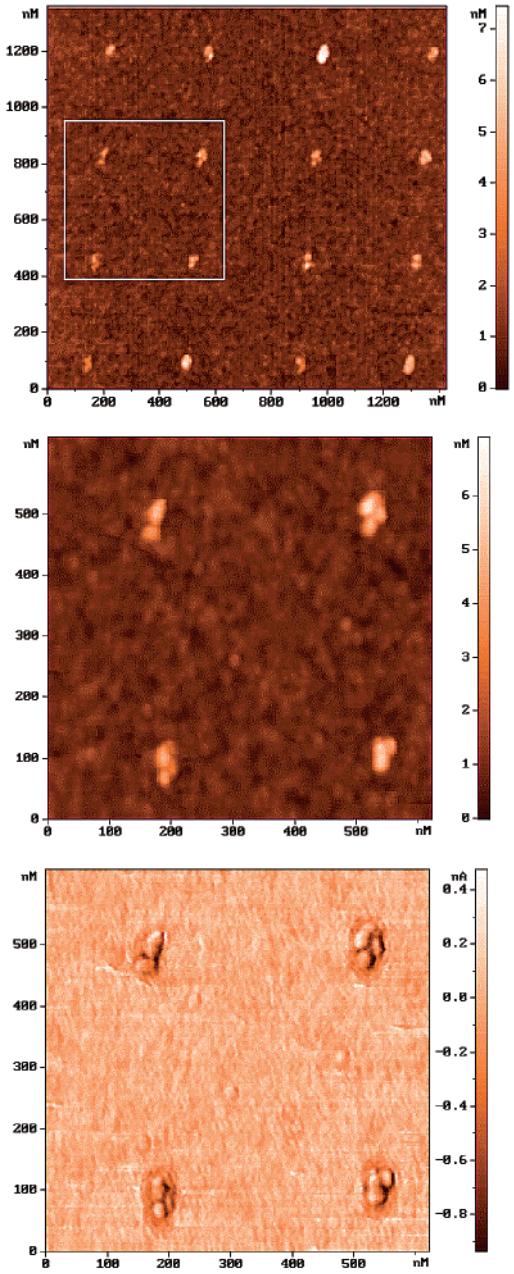

Figure 4. AFM semicontact mode images showing (top) an as-fabricated array of 16 [Au_{55}]/thiolated bilayer dots (topography), and simultaneously acquired topography (middle) and phase (bottom) enlarged scans of the marked four dots area after annealing at 80 °C for 12 hours (see text).

a 2D arrangement of wires connected to contact pads, with isolated metal clusters placed in predefined intrawire gaps, is shown in Figure 5 (e and f). Due to the particular experimental conditions and presumably sharper tip employed in the inscription of this pattern, it was possible to achieve here the desired assembly of a single gold cluster on each template dot, as well as that of wires made of single rows of gold clusters. This suggests that lateral confinement is indeed a major factor determining the mode of organization of the gold clusters on the template.

The template guided self-assembly of metal clusters demonstrated with the present preliminary results shows great

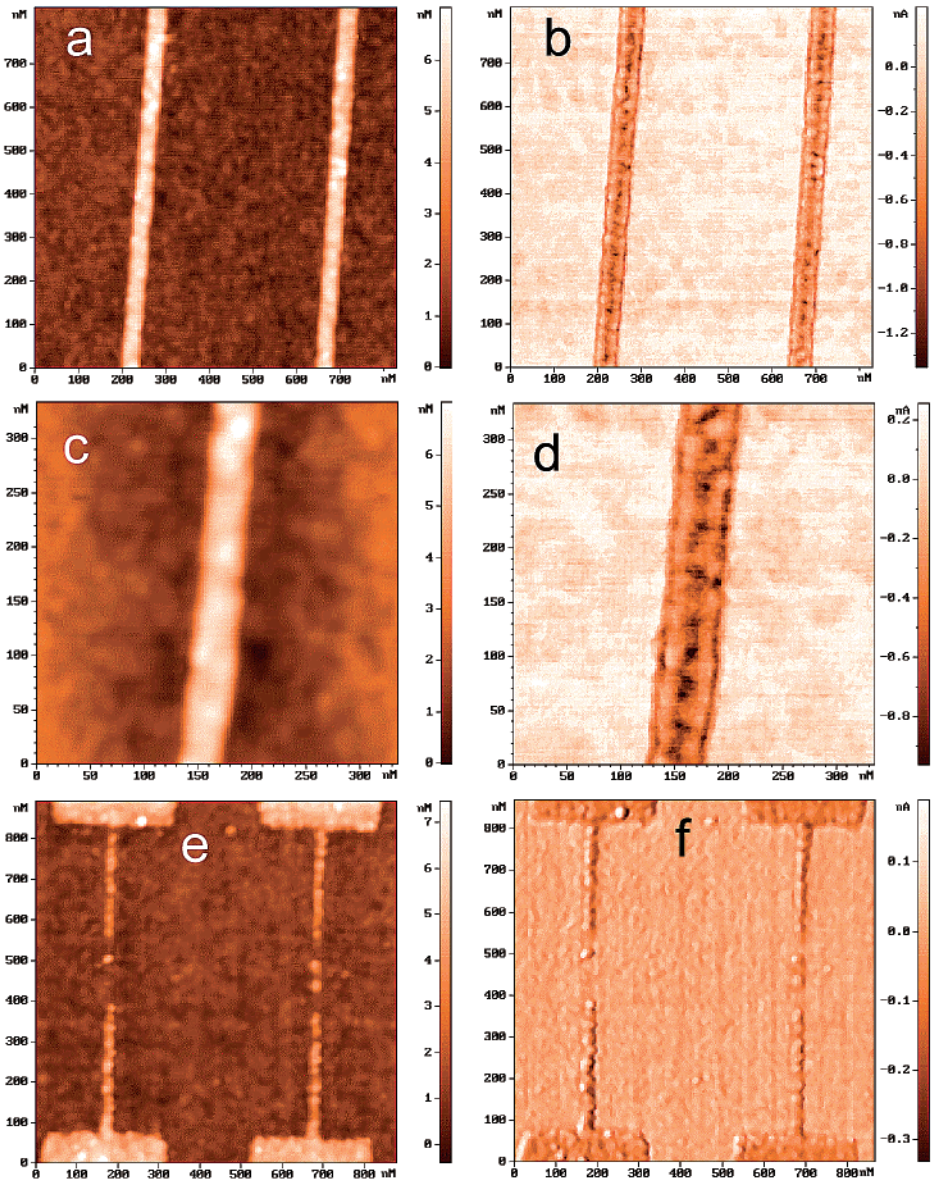

Figure 5. (a−d) Topography (left) and phase (right) AFM images (as in Figure 4) showing enlarged scans of portions of the [Au_{55}]-coated wires shown in Figure 2, before annealing. (e, f) Images as above (before annealing) of an enlarged portion of a [Au_{55}]/thiolated bilayer pattern combining dots, wires, and contact pads (see text). Note that the wires in images e and f were assembled on patterns inscribed in the raster mode, while in images a−d the initial pattern inscription was done in the vector mode.[14]

promise as a viable "bottom-up" approach to the realization of planned functional components for future nanodevices. To reach the level of control and reproducibility demanded for such applications, research efforts will have to be directed toward the basic understanding of the factors governing the tip-induced nanoelectrochemical patterning of monolayer surfaces and the mechanism of self-assembly on spatially confined template sites.

Acknowledgment. We thank Dr. Kazufumi Ogawa of Matsushita Electric Industrial Co. (Kyoto) for the supply of the NTS used in the assembly of the bilayer patterns, and Dr. Hagai Cohen of the Chemical Services Unit, WIS, for the XPS measurements. This research was supported by The Israel Science Foundation and Minerva Foundation (Germany).

References

(1) Ahmed, H. *J. Vac. Sci. Technol. B* **1997**, *15*, 2101−2108. Simon, U. *Adv. Mater*. **1998**, *10*, 1487−1492.
(2) Schmid, G. *Chem. Rev.* **1992**, *92*, 1709−1727. Simon, U.; Schön, G.; Schmid, G. *Angew. Chem., Int. Ed. Engl.* **1993**, *32*, 250−254.
(3) Chi, L. F.; Hartig, M.; Drechsler, T.; Schwaack, Th.; Seidel, C.; Fuchs, H.; Schmid, G. *Appl. Phys. A* **1998**, *66*, S187−S190.
(4) Schmid, G.; Bäumle, M.; Geerkens, M.; Heim, I.; Osemann, C.; Sawitowski, T. *Chem. Soc. Rev.* **1999**, *28*, 179−185.
(5) Schmid, G.; Chi, L. F. *Adv. Mater.* **1998**, *10*, 515−526.
(6) Schmid, G.; Bäumle, M.; Beyer, N. *Angew. Chem., Int. Ed.* **2000**, *39*, 181−183. Schmid, G.; Beyer, N. *Eur. J. Inorg. Chem.* **2000**, 835−837.
(7) Vidoni, O.; Reuter, T.; Torma, V.; Meyer-Zaika, W.; Schmid, G. *J. Mater. Chem.* **2001**, *11*, 3188−3190. Wyrwa, D.; Beyer, N.; Schmid, G. *Nano Lett.* **2002**, *2*, 419−421.
(8) Torma, V.; Reuter, T.; Vidoni, O.; Schumann, M.; Radehaus, Ch.; Schmid, G. *ChemPhysChem* **2001**, *8/9*, 546−548. Schmid, G.; Liu, Y.-P.; Schumann, M.; Raschke, Th.; Radehaus, Ch. *Nano Lett.* **2001**, *1*, 405−407.

(9) Maoz, R.; Cohen, S. R.; Sagiv, J. *Adv. Mater.* **1999**, *11*, 55−61. Maoz, R.; Frydman, E.; Cohen, S. R.; Sagiv, J. *Adv. Mater.* **2000**, *12*, 424−429.
(10) Maoz, R.; Frydman, E.; Cohen, S. R.; Sagiv, J. *Adv. Mater.* **2000**, *12*, 725−731.
(11) Hoeppener, S.; Maoz, R.; Cohen, S. R.; Chi, L. F.; Fuchs, H.; Sagiv, J. *Adv. Mater.* **2002**, *14*, 1036−1041.
(12) Schmid, G.; Meyer-Zaika, W.; Pugin, R.; Sawitowski, T.; Majoral, J.-P.; Caminade, A.-M.; Turrin, C.-O. *Chem. Eur. J.* **2000**, *6*, 1693−1697.
(13) Maoz, R.; Sagiv, J.; Degenhardt, D.; Möhwald, H.; Quint, P. *Supramol. Sci.* **1995**, *2*, 9−24. Baptiste, A.; Gibaud, A.; Bardeau, J. F.; Wen, K.; Maoz, R.; Sagiv, J. *Langmuir* **2002**, *18*, 3916−3922.
(14) The inscription of the patterns was done as before,[11] with a SOLVER P47 instrument (NT-MDT, Moscow, Russia) operated in the contact mode, in a controlled humidity atmosphere (∼60% relative humidity), using conductive W_2C-coated tips with normal spring constants of 0.5−2.0 N/m and an applied positive surface bias of 6−9 V relative to the tip. It was found that the patterning parameters should be separately optimized for the different produced features; with 400 raster-scanned points/line, patterns were inscribed by applying electrical pulses of 2.5−3.5 ms/point, at a bias of 9.0 V for dots, 8.4 V for wires, and 6.3 V for pads. Wires were also inscribed in the vector mode offered by the NT-MDT lithographic software, with pulses of 20−30 ms/point and a bias of 7.2 V.
(15) Frydman, E., Ph.D. Thesis, Weizmann Institute, September, 1999.
(16) Due to the high hydrophobicity of the unpatterned OTS background, the treated surface is not visibly wetted by either water or the gold solution. Weakly adhering surface contaminants, including gold particles accidentally left on unpatterned portions of the surface, could be lifted with a piece of Scotch tape. This surface cleaning treatment did not remove gold particles immobilized on the thiolated patterns and did not cause any damage to the fabricated structures.[10,11]
(17) The AFM images of the final gold-containing structures were acquired in the semicontact mode, with the SOLVER P47 instrument[11] equipped with regular (uncoated) silicon probes and operated in the ambient atmosphere.
(18) It should be noted that semicontact mode phase images exaggerate lateral dimensions more than the corresponding topographic images. On the other hand, such images offer significantly improved resolution (see Figures 3−5).
(19) Lindsay, S. M. In *Scanning Probe Microscopy and Spectroscopy Second Edition*; Bonnell, D. A., Ed.; Wiley-VCH: New York, 2001; pp 289−335. Burnham, N. A.; Colton, R. J. In *Scanning Probe Microscopy and Spectroscopy Second Edition*; Bonnell, D. A., Ed.; Wiley-VCH: New York, 2001; pp 337−369.
(20) Schmid, G.; Pugin, R.; Sawitowski, T.; Simon, U.; Marler, B. *Chem. Commun.* **1999**, 1303−1304.

NL025659C